

## Chapter 8: Channel and Pipe Flow (Chap. 7 Bernard)

### Part 2: Pipe Flow

$Re \sim 2000$  transition turbulence.

$$Re = \frac{U_m D}{\nu} \quad U_m = \frac{Q}{A}$$

Fully developed flow:  $\underline{\bar{U}} = (\bar{U}(r), 0, 0) \rightarrow$  averaged streamwise momentum equation:

$$0 = -\frac{\partial \bar{p}}{\partial x} + \frac{1}{r} \frac{d}{dr} \left( \mu r \frac{d\bar{U}}{dr} - \rho r \overline{uv_r} \right) \quad (1)$$

Where  $r$  is the outward radial coordinate, i.e.,  $r = 0$  at the center of the pipe and  $r = R_0$  at the wall. Introduce wall coordinate:

$$y \equiv R_0 - r$$

Such that:

$$\bar{U}^*(y) = \bar{U}(R_0 - y)$$

However, the  $*$  symbol will be dropped.

The wall shear stress:

$$\tau_w = \mu \frac{d\bar{U}}{dy}(0)$$

Which also defines  $R_\tau = \frac{U_\tau D}{\nu}$  where  $U_\tau = \sqrt{\frac{\tau_w}{\rho}}$  = friction velocity.

Integrating Eq. (1) over the pipe cross-section yields

$$\begin{aligned}
 0 &= \int_0^{R_0} \int_0^{2\pi} -\frac{\partial \bar{p}}{\partial x} + \frac{1}{r} \frac{d}{dr} \left( \mu r \frac{d\bar{U}}{dr} - \rho r \overline{uv_r} \right) r dr d\theta \\
 0 &= -\pi R_0^2 \frac{\partial \bar{p}}{\partial x} - 2\pi R_0 \tau_w \\
 -\pi R_0^2 \frac{\partial \bar{p}}{\partial x} &= 2\pi R_0 \tau_w \quad (2)
 \end{aligned}$$

Since

$$\frac{d\bar{U}}{dr}(R_0) = -\frac{d\bar{U}}{dy}(0)$$

And

$$\overline{v_r}(0) = \overline{uv_r}(0) = \overline{uv_r}(R_0) = 0$$

Eq. (2) shows that  $\frac{\partial \bar{p}}{\partial x} = f(\tau_w)$ .

The volumetric flow rate:

$$Q = 2\pi \int_0^{R_0} \bar{U}(r) dr$$

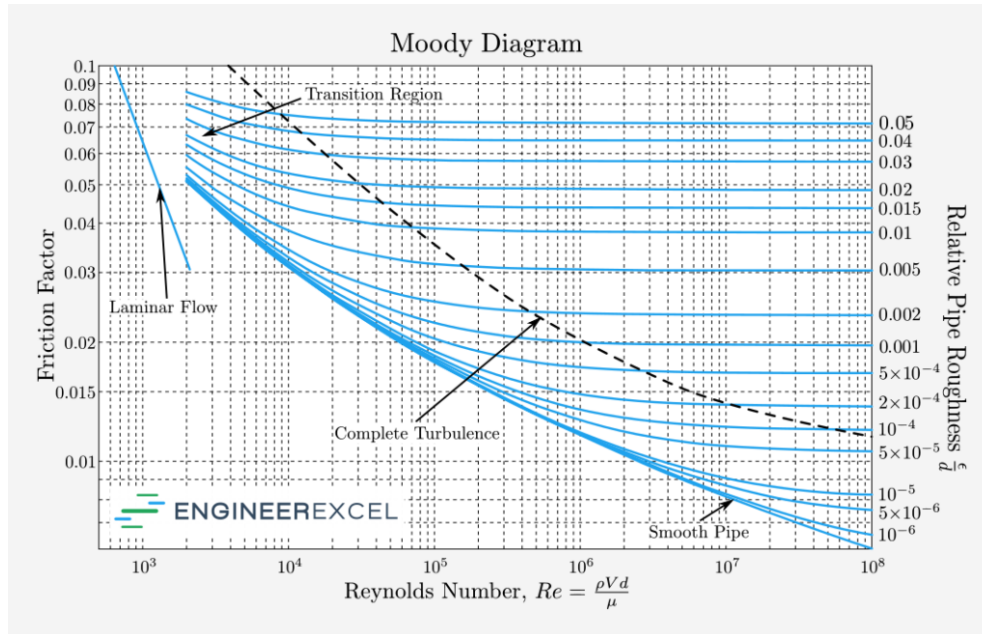
can be determined once  $\bar{U}(r)$  is known, which determines the averaged velocity  $U_m = Q/A$  where  $A = \pi R_0^2$  and defines the Reynolds number

$$Re = \frac{U_m D}{\nu}$$

Define friction factor for pipe flow  $f$  as:

$$f = \frac{\Delta \bar{p}}{\Delta x} \frac{2D}{\rho U_m^2} = 8 \frac{R_\tau^2}{R_e^2} = \frac{8\tau_w}{\rho U_m^2} \quad (3)$$

The Moody diagram can be used to find values of  $f(Re)$ .



Current analysis presumes that the pipe is smooth. For engineering applications, it is necessary to consider  $f(Re, \frac{\epsilon}{d})$ , where  $\frac{\epsilon}{d}$  represents the relative pipe roughness.

Alternatively explicit formulas are available for smooth and rough pipes, e.g.:

For  $Re < 10^5$ , the Blasius smooth pipe friction law

$$f = 0.266 Re^{-1/4}$$

And substituting this into Eq. (3) gives a relationship between  $R_\tau$  and  $R_e$

$$R_\tau = 0.182 Re^{7/8}$$

Previous channel flow analysis neglected outer layer, which should be included for pipe and especially BL flows.

In viscous sublayer ( $y^+ < 5$ ):

$$\overline{U}^+ = y^+$$

And log law valid for intermediate layer of pipe flow:  $\overline{U}^+ = \frac{1}{\kappa} \ln y^+ + B$ .

For high Re pipe flow, central core mean velocity cannot be scaled using viscosity, so similarity is achieved using the velocity defect law:

$$\frac{\overline{U}_{cl} - \overline{U}(y)}{U_\tau} = g(\xi)$$

Where  $\overline{U}_{cl}$  = mean centerline velocity and  $\xi \equiv y/R_0$  is a similarity variable. In practice, this equation is found to work also in most of the intermediate region.

If velocity defect law applies in overlap region, then:

$$f(y^+) = \overline{U}^+ = \frac{\overline{U}_{cl}}{U_\tau} - g(\xi) \quad (4)$$

Differentiating Eq. (4) with respect to  $y$  gives

$$\frac{df}{dy^+}(y^+) \frac{U_\tau}{\nu} = -\frac{dg}{d\xi}(\xi) \frac{1}{R_0}$$

$$y^+ = \frac{U_\tau y}{\nu}$$

And multiplying both sides of the equation by  $y$  gives:

$$y^+ \frac{df}{dy^+}(y^+) = -\xi \frac{dg}{d\xi}(\xi) \quad (5)$$

LHS only  $f(y^+)$  and RHS only  $f(\xi)$ ; thus, both sides must be equal and constant. Setting the constant to be  $1/k$ :

$$y^+ \frac{df}{dy^+}(y^+) = \frac{1}{k}$$

Integration gives the log law:

$$\overline{U}^+ = k^{-1} \log y^+ + B$$

i.e., using velocity defect law in intermediate layer recovers log-law.

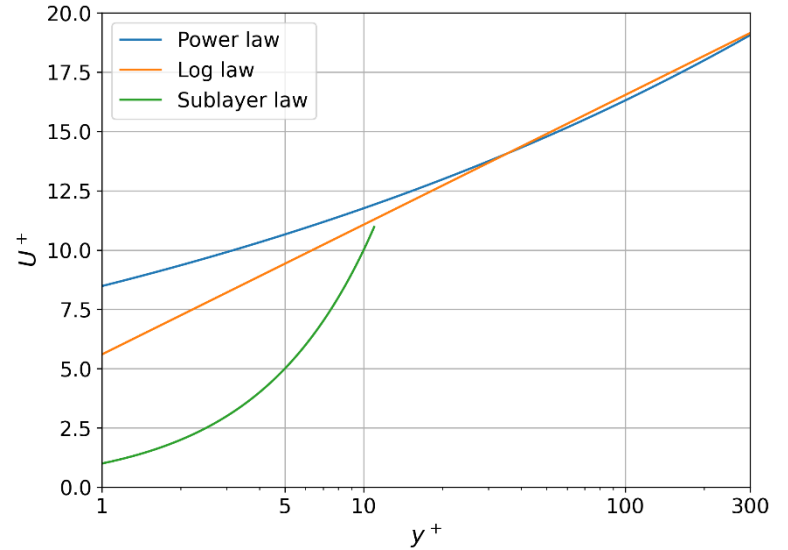
New high Re data shows  $k = 0.42$ ,  $B = 5.6$  for  $600 \leq y^+ \leq 0.12R_0^+$  vs. historical 0.41 and 5.2.

The details of the velocity defect law for outer flow will be analyzed for BL flow.

In the region beyond the viscous sublayer, up to  $y^+ \sim 300$ , a power law gives:

$$\bar{U}^+ = 8.48(y^+)^{0.142}$$

For  $5 < y^+ < 300$ .



When compared with previously defined composite sub-layer, blending layer, and logarithmic-overlap formula

$$U^+ = y^+ - e^{-\kappa B} \left[ e^{\kappa U^+} - 1 - \kappa U^+ - \frac{(\kappa U^+)^2}{2} - \frac{(\kappa U^+)^3}{6} \right]$$

Shows its limitations.

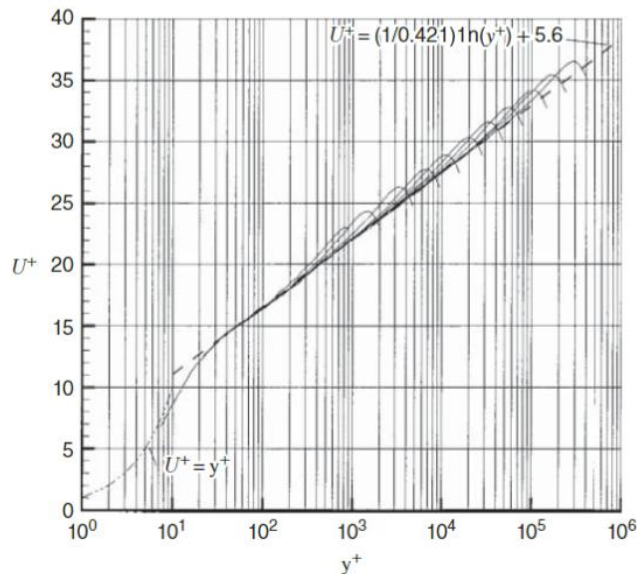


Figure 7.18 Mean velocity profiles in pipe flow [6] showing the collective approach to a log law. The curves are for Reynolds numbers between  $R_e = 31 \times 10^3$  and  $R_e = 18 \times 10^6$ . Reprinted with permission of Cambridge University Press.

## Power Law

Early studies showed that power laws can represent flow behavior over the entire pipe cross-section:

$$\frac{\bar{U}}{U_{cl}} = \left(\frac{y}{R_0}\right)^{1/n}$$

Where  $n$  increases with  $Re$ , shows good fit with data, but cannot provide  $\tau_w$ .

Taking a derivative of the power law gives:

$$\frac{d\bar{U}}{dy} = \frac{U_{cl}}{n} \left(\frac{y}{R_0}\right)^{\frac{1}{n}-1}$$

Where experimental fits show that  $n \sim 6 - 10$ , such that  $\frac{1}{n} - 1 \sim - (0.85 - 0.9)$ .

Therefore, e.g., for  $n = 10$ :

$$\frac{d\bar{U}}{dy}(0) \sim \frac{U_{cl}}{n} \left(\frac{R_0}{y}\right)^{0.9}$$

Showing that the shear stress approaches  $\infty$  as  $y \rightarrow 0$ .

Linear-log plots of power law show good fit to the data for range of  $n$ :

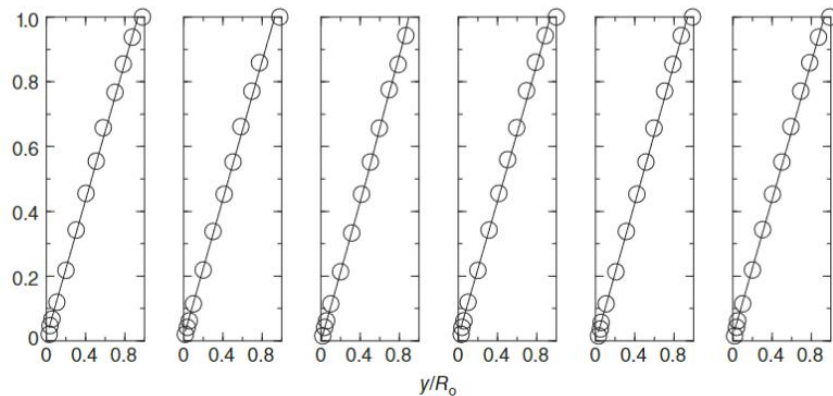


Figure 7.19 Plots of  $(\bar{U}/\bar{U}_{max})^{1/n}$  in pipe flow for empirically fitted exponents,  $n$ . From left to right  $n = 6.0, 6.6, 7.0, 8.8, 10.0$ , and the Reynolds numbers are  $4 \times 10^3, 2.3 \times 10^4, 1.1 \times 10^5, 1.1 \times 10^6, 2 \times 10^6$ , and  $3.2 \times 10^6$ . From [25], p. 563.

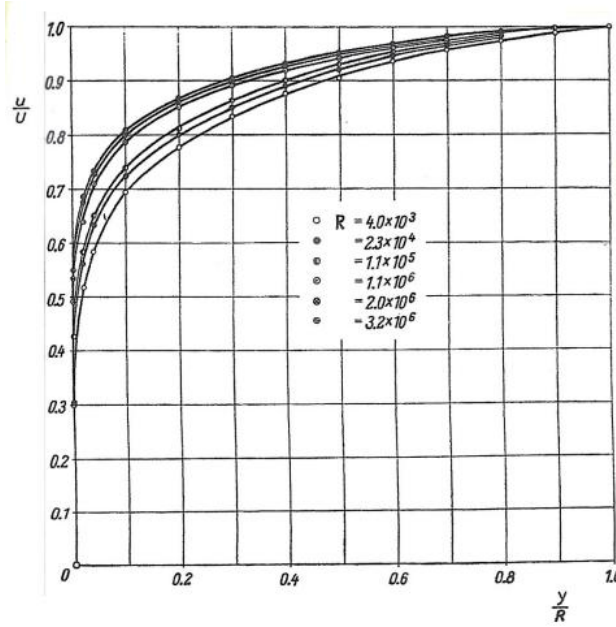


Fig. 20.2. Velocity distribution in smooth pipes for varying Reynolds number, after Nikuradse [45]

Subsequently, power laws were generalized to include not only inner law variables ( $y, \tau_w, \nu, \rho$ ) but also outer law variable  $R_0$ , i.e.,  $d\bar{U}/dy = f(y, \tau_w, \nu, \rho, R_0)$  for the intermediate layer to include dependence on  $\nu$  and  $R_0$ , i.e., generalization of the log law approach, but in this case not independent of  $Re$  (partial similarity).

Dimensional analysis gives:

$$\frac{d\bar{U}}{dy} = \frac{U_\tau}{y} f(y^+, R_\tau) \quad (6)$$

But since  $R_\tau$  is related to  $R_e$ , Eq. (6) can be rewritten as:

$$\frac{d\bar{U}}{dy} = \frac{U_\tau}{y} f(y^+, R_e) \quad (7)$$

If  $f = \text{constant}$ , log law is implied, alternatively if  $f$  obeys a power law:

$$f(y^+, R_e) = \beta^*(R_e)(y^+)^{\alpha(R_e)} \quad (8)$$

For large  $y^+$  and  $R_e$ .



Both  $\bar{U}^+$  and  $f$  will follow power laws after integration of Eq. (7) using (8).

$$\begin{aligned}
 d\bar{U} &= \frac{U_\tau}{y} \beta^*(R_e) (y^+)^{\alpha(R_e)} dy \\
 d\bar{U}^+ &= \beta^* (y^+)^{\alpha-1} dy^+ \\
 \int_{\bar{U}^+(0)}^{\bar{U}^+(y^+)} d\bar{U}^+ &= \beta^* \int_0^{y^+} (y^+)^{\alpha-1} dy^+
 \end{aligned}$$

$$\begin{aligned}
 y^+ &= \frac{U_\tau y}{\nu} \\
 dy^+ &= \frac{U_\tau}{\nu} dy \\
 \bar{U}^+ &= \frac{\bar{U}}{U_\tau}
 \end{aligned}$$

Applying BC at the wall gives:

$$\bar{U}^+(y^+) = \frac{\beta^*}{\alpha} (y^+)^{\alpha}$$

$$\bar{U}^+(y^+) = \beta(R_e) (y^+)^{\alpha(R_e)} \quad (9)$$

Where  $\beta$  is defined from  $\alpha$  and  $\beta^*$  after the integration, i.e.,  $\beta = \beta^* / \alpha$ .

To determine a form of  $\alpha(R_e)$ , consider behavior of Eq. (9) as  $\nu \rightarrow 0$ . If  $\frac{\partial \bar{p}}{\partial x}$  is constant,  $\tau_w$  remains constant as  $\nu \rightarrow 0$ , and so does  $U_\tau$ , as per Eq. (2).

Since  $\bar{U}$  is bounded,  $\bar{U}^+$  is bounded, so LHS of Eq. (9) is bounded as  $\nu \rightarrow 0$ .

Consequently, RHS must be bounded as  $y^+ \rightarrow \infty$  and  $R_e \rightarrow \infty$ .

Noting the identity

$$(y^+)^{\alpha(R_e)} = e^{\alpha(R_e) \log y^+}$$

Eq. (9) can be rewritten as:

$$\bar{U}^+(y^+) = \beta(R_e) e^{\alpha(R_e) \log y^+}$$

$\alpha(R_e)$  is assumed of the form:

$$\alpha(R_e) = \frac{\alpha_1}{\log R_e}$$

Such that:

$$\overline{U}^+(y^+) = \beta(R_e)(y^+)^{\frac{\alpha_1}{\log R_e}}$$

and gives good agreement with experiments. It is assumed that  $\beta(R_e)$  shows the same dependence on  $R_e$  as  $\alpha$ :

$$\beta(R_e) = \beta_0 + \frac{\beta_1}{\log R_e}$$

Where  $\beta_0$  and  $\beta_1$  are constants.

It is then derived that:

$$\overline{U}^+(y^+) = \left( \beta_0 + \frac{\beta_1}{\log R_e} \right) (y^+)^{\frac{\alpha_1}{\log R_e}} \quad (10)$$

Where the appearance of  $R_e$  in the form of its logarithm means that if  $R_e$  is replaced by  $\gamma R_e \rightarrow \log \gamma R_e = \log \gamma + \log R_e$ , which converges to  $\log R_e$  as  $R_e \rightarrow \infty$ .

$\alpha_1$  and  $\beta_1$  should have universal form and together with  $\beta_0$  are determined by empirical fit, comparing with EFD data.

For  $4 \times 10^3 \leq R_e \leq 3.24 \times 10^6$ :  $\alpha_1 = 1.5$ ,  $\beta_0 = 0.578$ , and  $\beta_1 = 2.5$ .

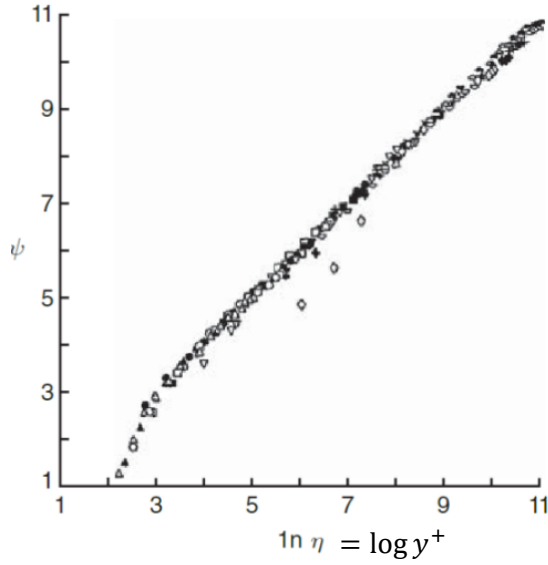


**Figure 7.20**  $\psi$  vs.  $\log y^+$  where  $\eta \equiv y^+$  in this figure. Data are taken from 16 different Reynolds numbers from  $4 \times 10^3$  to  $3.24 \times 10^6$  measured in [29]. From [31]. Reprinted with permission from ASME International.

$$\psi \equiv \frac{\log R_e}{\alpha_1} \log \left( \frac{\bar{U}^+}{\beta_0 + \frac{\beta_1}{\log R_e}} \right)$$

From Eq. (10):

$$\frac{\bar{U}^+}{\beta(R_e)} = (y^+)^{\frac{\alpha_1}{\log R_e}} = a$$

$$\log a = \frac{\alpha_1}{\log R_e} \log y^+ \rightarrow \log y^+ = \frac{\log R_e}{\alpha_1} \log a = \psi$$

i.e., Eq. (10) is equivalent to  $\psi = \log y^+$ .

Since the power law is meant to cover larger region of the pipe than the log law, it can be used to explain large  $y^+$  departure from log law.

### Pope 7.3.4

In the overlap region ( $\nu/U_\tau \ll y \ll \delta$ ) two velocities profiles are possible, i.e., the log law:

$$u^+ = \frac{1}{k} \log y^+ + B$$

And the power law:

$$u^+ = C(y^+)^{\alpha}$$

The coefficients  $k, B, \alpha$ , and  $C$  can be  $f(R_e)$ . If that's not the case, the laws are said to be universal.

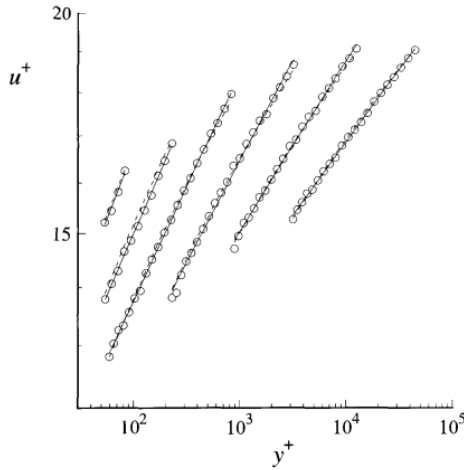


Fig. 7.31. A log-log plot of mean velocity profiles in turbulent pipe flow at six Reynolds number (from left to right:  $Re \approx 32 \times 10^3$ ,  $99 \times 10^3$ ,  $409 \times 10^3$ ,  $1.79 \times 10^6$ ,  $7.71 \times 10^6$ , and  $29.9 \times 10^6$ ). The scale for  $u^+$  pertains to the lowest Reynolds number; subsequent profiles are shifted down successively by a factor of 1.1. The range shown is the overlap region,  $50\delta < y < 0.1R$ . Symbols, experimental data of Zagarola and Smits (1997); dashed lines, log law with  $\kappa = 0.436$  and  $B = 6.13$ ; solid lines, power law (Eq. (7.157)) with the power  $\alpha$  determined by the best fit to the data.

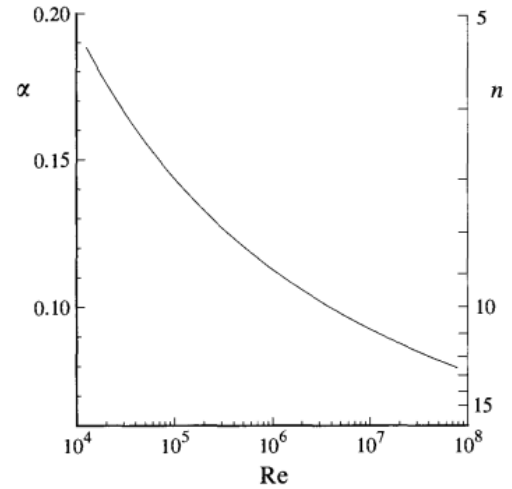
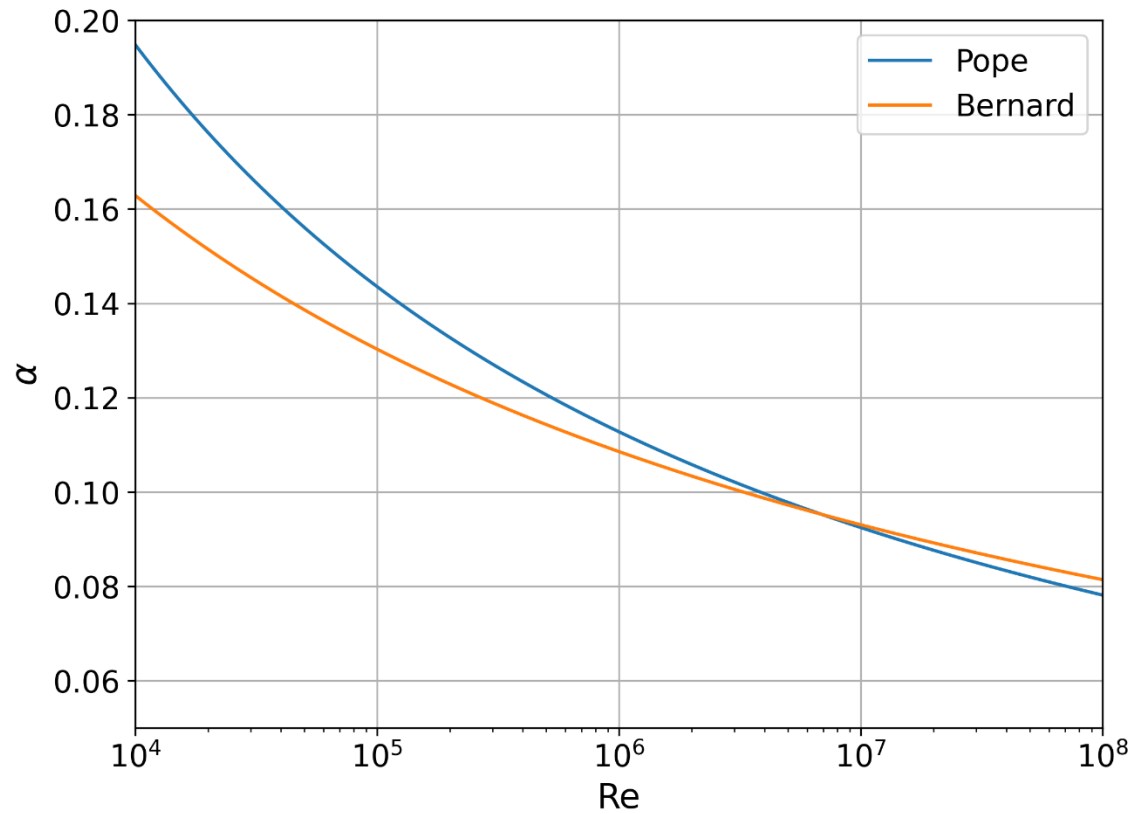


Fig. 7.32. The exponent  $\alpha = 1/n$  (Eq. (7.158)) in the power-law relationship  $u^+ = C(y^+)^{\alpha} = C(y^+)^{1/n}$  for pipe flow as a function of the Reynolds number.

It is clear that  $\alpha$  decreases significantly with  $R_e$ . An empirical formula is given by:

$$\alpha = \frac{1.085}{\log R_e} + \frac{6.535}{(\log R_e)^2}$$

Vs Bernard  $\alpha = \frac{\alpha_1}{\log R_e} = \frac{1.5}{\log R_e}$



Streamwise normal RS  $\overline{u^2}$  for high Re data shows 2<sup>nd</sup> peak in addition to peak at  $y^+ = 15$ , but reason for this is still under discussion.

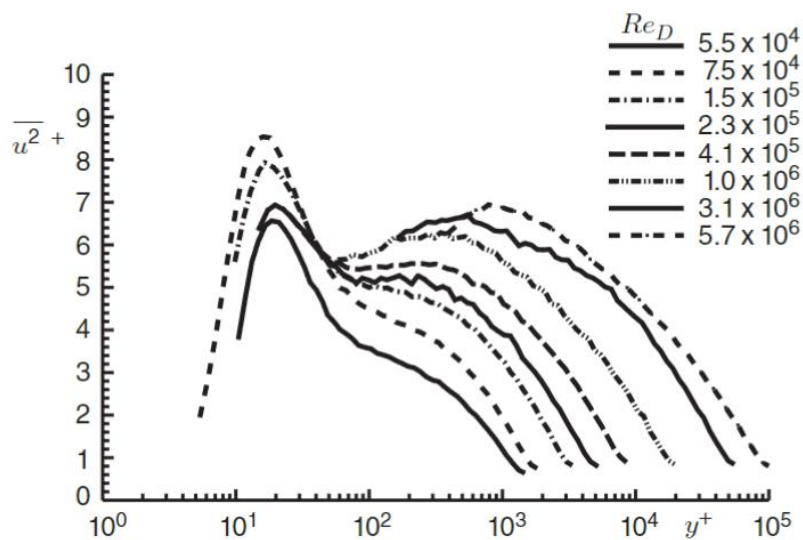


**Figure 7.21** Streamwise velocity variance at high Reynolds numbers in pipe flow [32]. Reprinted with permission of Cambridge University Press.

## Appendix

Roughness

$$k = \text{roughness height}$$

$$k^+ = \frac{k u^*}{\nu}$$

 $k^+ < 4$  hydraulically smooth $4 < k^+ < 60$  transitional roughness  $f(Re)$  $k^+ > 60$  fully rough  $\neq f(Re)$ 

$$\sigma/u^* = \frac{1}{\kappa} \ln y^+ + B + \frac{2\pi}{\kappa} W(y^+/s) - \Delta U^+$$

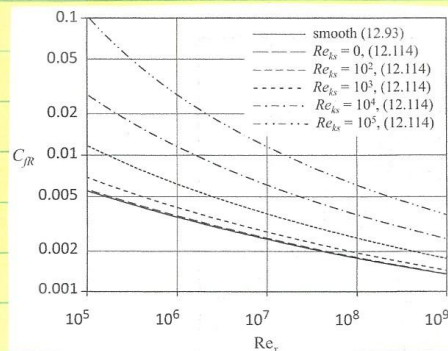
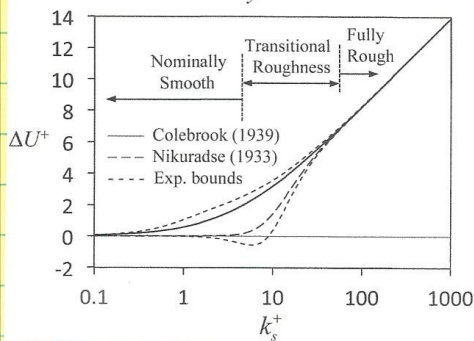
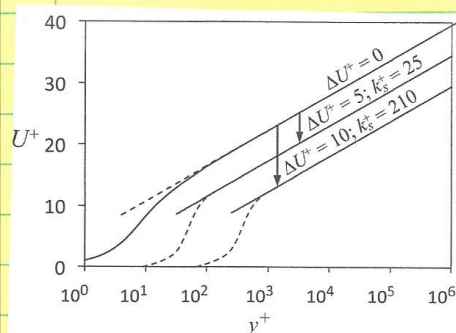
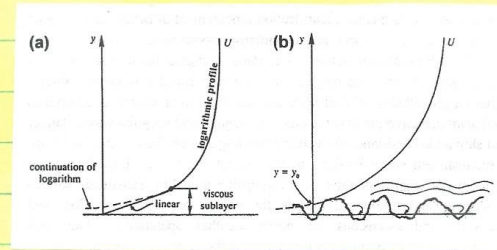


**FIGURE 12.25** Rough surface skin friction coefficient,  $C_{fR}$ , for a zero-pressure-gradient flat-plate turbulent boundary layer vs.  $Re_x$ , the Reynolds number based on downstream distance. The solid curve corresponds to (12.93) evaluated using log-law constants  $\kappa=0.39$  and  $B=4.3$  (as recommended by Marusic et al., 2013). The dashed and dash-dot curves come from implicit evaluation of (12.114) for equivalent-sand-grain roughness-height Reynolds numbers of  $Re_{ks} = 0, 10^2, 10^3, 10^4$ , and  $10^5$ . The  $C_{fR}$  values produced by (12.114) agree within engineering accuracy ( $\pm 5\%$  or so) with prior rough-plate results.